Cell

Article

Paternal Diet Defines Offspring Chromatin State and Intergenerational Obesity

Anita Öst,[1,6,8,*] Adelheid Lempradl,[1,8] Eduard Casas,[2,3] Melanie Weigert,[1] Theodor Tiko,[1] Merdin Deniz,[1] Lorena Pantano,[2] Ulrike Boenisch,[1] Pavel M. Itskov,[7] Marlon Stoeckius,[4] Marius Ruf,[1] Nikolaus Rajewsky,[4] Gunter Reuter,[5] Nicola Iovino,[1] Carlos Ribeiro,[7] Mattias Alenius,[6] Steffen Heyne,[1] Tanya Vavouri,[2,3] and J. Andrew Pospisilik[1,*]

[1]Max Planck Institute of Immunobiology and Epigenetics, Stuebeweg 51, 79108 Freiburg, Germany
[2]Institut de Medicina Predictiva i Personalitzada del Càncer, Can Ruti Campus, Ctra. de Can Ruti, Camí de les Escoles s/n, 08916 Badalona, Barcelona, Spain
[3]Josep Carreras Leukaemia Research Institute (IJC), ICO-Hospital GermansTrias i Pujol, 08916 Badalona, Barcelona, Spain
[4]Systems Biology of Gene Regulatory Elements, Max-Delbrück-Center for Molecular Medicine, Robert-Rössle-Strasse 10, 13125 Berlin, Germany
[5]Institute of Biology, Developmental Genetics, Martin Luther University Halle, 06120 Halle, Germany
[6]Department of Clinical and Experimental Medicine, Linkoping University, 58183 Linkoping, Sweden
[7]Champalimaud Neuroscience Programme, Champalimaud Centre for the Unknown, 1400-038 Lisbon, Portugal
[8]Co-first author
*Correspondence: anita.ost@liu.se (A.Ö.), pospisilik@ie-freiburg.mpg.de (J.A.P.)
http://dx.doi.org/10.1016/j.cell.2014.11.005

SUMMARY

The global rise in obesity has revitalized a search for genetic and epigenetic factors underlying the disease. We present a *Drosophila* model of paternal-diet-induced *i*ntergenerational *m*etabolic *r*eprogramming (IGMR) and identify genes required for its encoding in offspring. Intriguingly, we find that as little as 2 days of dietary intervention in fathers elicits obesity in offspring. Paternal sugar acts as a physiological suppressor of variegation, desilencing chromatin-state-defined domains in both mature sperm and in offspring embryos. We identify requirements for H3K9/K27me3-dependent reprogramming of metabolic genes in two distinct germline and zygotic windows. Critically, we find evidence that a similar system may regulate obesity susceptibility and phenotype variation in mice and humans. The findings provide insight into the mechanisms underlying intergenerational metabolic reprogramming and carry profound implications for our understanding of phenotypic variation and evolution.

INTRODUCTION

Global incidence of obesity is approaching 1 billion humans. Though poorly understood, parental and fetal nutritional states have been shown to generate reproducible offspring phenotypes, including obesity. Studies in multiple model organisms have been used to examine intergenerational metabolic effects (Braunschweig et al., 2012; Ozanne et al., 1999; Morgan et al., 1999; Buescher et al., 2013; Rechavi et al., 2014). Maternal and paternal induction of intergenerational responses have been reported, and a variety of macronutrient and timing interventions have been used, including short- and long-term fasting (Anderson et al., 2006), calorie restriction (Blondeau et al., 2002; Jimenez-Chillaron et al., 2009), and modulation of dietary protein (Ozanne et al., 1999), fat (Gniuli et al., 2008; Dunn and Bale, 2009), and methyl-donor content (Wolff et al., 1998; Waterland et al., 2006; reviewed in Daxinger and Whitelaw, 2012; Patti, 2013). Of note, although not understood, divergent physiological extremes can prompt similar offspring phenotypes, so called "U-shaped" responses.

Intergenerational effects transmitted via the male germline have received recent attention. Because father-to-offspring transmission excludes difficult to control oocyte and gestational effects, mechanistic dissections are simplified. Studies have demonstrated paternal transmission of tumor susceptibility (Anway et al., 2005; Xing et al., 2007), of heat-shock-induced epigenetic memory (Seong et al., 2011), of olfaction-dependent behavioral and neural phenotypes (Dias and Ressler, 2014), and of metabolic control (Anderson et al., 2006; Fullston et al., 2013; Carone et al., 2010; Ng et al., 2010; reviewed in Rando, 2012).

Mechanistically, imprinting, altered DNA methylation, histone modifications, and noncoding RNA transcripts have been implicated in inter/transgenerational phenotype transmission. Adiposity of genetically identical agouti mouse siblings correlates with IAP DNA methylation (Morgan et al., 1999); DNA methylation correlates with endocrine disruptor and nutrient induced inter/transgenerational phenotypes (Anway et al., 2005; Carone et al., 2010; Radford et al., 2014), and there is evidence of RNA-dependent transmission (Gapp et al., 2014; Rechavi et al., 2014; Kiani et al., 2013; Rassoulzadegan et al., 2006). In *C. elegans* and *Drosophila*, research has focused on small noncoding RNAs and chromatin organization (Seong et al., 2011; Shirayama et al., 2012; Lee et al., 2012; Greer et al., 2011; Ashe et al., 2012). Despite these advances, however, our understanding of the initiation, transmission, and stabilization of trans/intergenerational phenotypes remains largely a black box.

Here, we present a *Drosophila* model of paternal *i*ntergenerational *m*etabolic *r*eprogramming (IGMR) and identify

germline and zygotic gene networks that are necessary for its manifestation. Mechanistically, paternal sugar modifies offspring chromatin state and transcription in a *Polycomb*-, *E(z)*-, *SetDB1*-, *Su(var)3-9*-, and *HP1*-sensitive manner. Intriguingly, these changes are forecast in the sperm. Data from highly defined human and mouse obesity cohorts suggest that these processes are conserved. These data provide evidence for a conserved chromatin-state-encoded program that defines phenotypic variation and thus carry profound implications for our understanding of phenotypic diversity and evolution.

RESULTS

A *Drosophila* Model of Intergenerational Metabolic State Control

We sought to understand whether normal fluctuations in diet might impact next-generation phenotypes. We chose to focus on the male germline and, for simplicity, on male progeny.

To minimize genetic variation, we performed ten generations of single-fly, brother-sister inbreeding of our population inbred w^{1118} *Drosophila melanogaster* strain. To identify an optimal dietary intervention for P0 fathers, we challenged 4- to 5-day-old males with progressively increasing dietary sugar and protein and assessed whole-fly fat storage after 2 days. Whereas dietary protein showed minimal effects (Figure 1A; horizontal axis), dietary sugar evoked a 3-fold increase in whole-fly triglyceride storage (Figure 1A; vertical axis). Of note, the sugar concentrations used approximate natural food sources (ripened banana ~300 g/l). These responses agreed with published data (Skorupa et al., 2008) and highlighted the rapid metabolic regulatory potential of dietary sugar in the fly.

To test for intergenerational effects, we repeated the experiment, this time varying only sugar, and mated the males to standardized w^{1118} female virgins (Figure 1B). After 2 hr of mating, females were left to lay eggs for 10 hr, removed, and the F1 offspring were left to develop unimpeded. Importantly, ancestral (more than ten generations), parental, and F1 generations were highly controlled with respect to male:female mating ratio, larval density, diet, and environmental conditions. One week after eclosure, adult male offspring were weighed and sacrificed, and triglyceride levels were measured in whole-fly lysates. Interestingly, although the paternal intervention showed no effect on F1 kept on normal food (Figure 1C, top, open circles), adult progeny fed an obesogenic high-sugar diet exhibited a U-shaped obesity response (Figure 1C, top closed circles) with low- and high-sugar sired individuals showing exaggerated triglycerides (Figure 1C and 1D). This phenotype was significant by both ANOVA and comparison of linear versus polynomial regressions. Thus, paternal sugar outside of the physiological optimum alters metabolic control in the F1.

The IGMR phenotype comprised two features. F1 offspring body weight increased with paternal sugar (Figure 1C, middle), and weight-normalized triglyceride levels increased toward both paternal extremes (Figure 1C and 1D). Metabolic phenotyping revealed that obesity-susceptible IGMR progeny exhibited increased adipose area (Figure 1E and 1F) and lipid droplet size (Figure 1E and Figure S1A available online). Measures of feeding behavior showed a tendency toward increased food intake (Figure 1G). Together with increased starvation sensitivity (Figure S1D), unaltered activity and CO_2 production measures (Figures S1B and S1C), as well as unaltered trehalose and glucose levels (Figures S1E and S1F), these findings suggest that the observed excess triglyceride reserves resulted from poor lipid store mobilization and possibly hyperphagia. Importantly, we found no evidence of altered ecclosure timing (Figure 1H) or wing size (Figure 1I, top), or in F1 offspring number (Figure 1I, middle) or male:female ratio per brood (Figure 1I, bottom). Thus, acute paternal dietary sugar reprograms offspring metabolism, leaving growth and development intact. Our data conclusively provide evidence that acute paternal diet reprograms offspring metabolism in *Drosophila*.

Paternal IGMR Is Rapid, Stable, and Stress Sensitive

The short 2 day intervention implied that mature *Drosophila* sperm are capable of continuously transmitting environmental cues to their offspring. To understand the minimum dietary intervention required to elicit paternal IGMR, w^{1118} males were subject to dietary interventions lasting 1, 2, 5, or 7 days prior to mating (Figure 2A). Measurements of adiposity indicated a maximal F1 phenotypic response within just 2 days of paternal challenge (Figures 2B and 2C), suggesting that paternal IGMR might be detectable within a single day. Female flies store sperm upon mating, allowing them to fertilize eggs for days or even weeks after a single insemination event. We asked how stable the IGMR phenotype would be with sperm storage. Males were subject to a 2 day paternal dietary intervention and mated, and the recipient females were allowed to lay three consecutive batches of fertilized eggs over 60 hr. Importantly, offspring of all three consecutive batches exhibited clear U-shaped obesity phenotypes (Figures 2D and 2E), indicating that IGMR is stable with sperm storage. Further, heat shock is known to modulate epigenetically controlled phenotypes, even across generations (Seong et al., 2011). Interestingly, a 1 hr heat shock of diet-treated fathers immediately before mating completely abrogated the paternal IGMR obesity response (Figures 2F and 2G). This is consistent with the requirement for highly controlled environmental conditions (sound, odor, vibration) when using this model. Finally, we found no evidence that the IGMR phenotype is transmitted to subsequent generations (Figure 2H). Thus, paternal IGMR is rapid, stable, and acutely stress sensitive.

Paternal Sugar Alters Offspring Heterochromatin

Paternal IGMR appeared phenotypically "silent" through the complexities of development. We therefore hypothesized that the phenotype was encoded in chromatin. Position-effect variegation (PEV) is a genetic phenomenon that has been used as a quantitative readout of locus-specific chromatin state silencing in vivo. The most common PEV reporters in *Drosophila* reflect chromatin desilencing through increased expression of a red-eye-pigment-coding reporter gene. Screening a library of PEV strains, Phalke and colleagues recently defined at least five functionally distinct chromatin silencing subtypes in the living fly (Phalke et al., 2009). Using identical or comparable PEV lines, we tested whether paternal dietary sugar could alter offspring eye color and thus stably alter chromatin state in F1 (Figures 3A–3E). We observed no overt effect of paternal diet on offspring

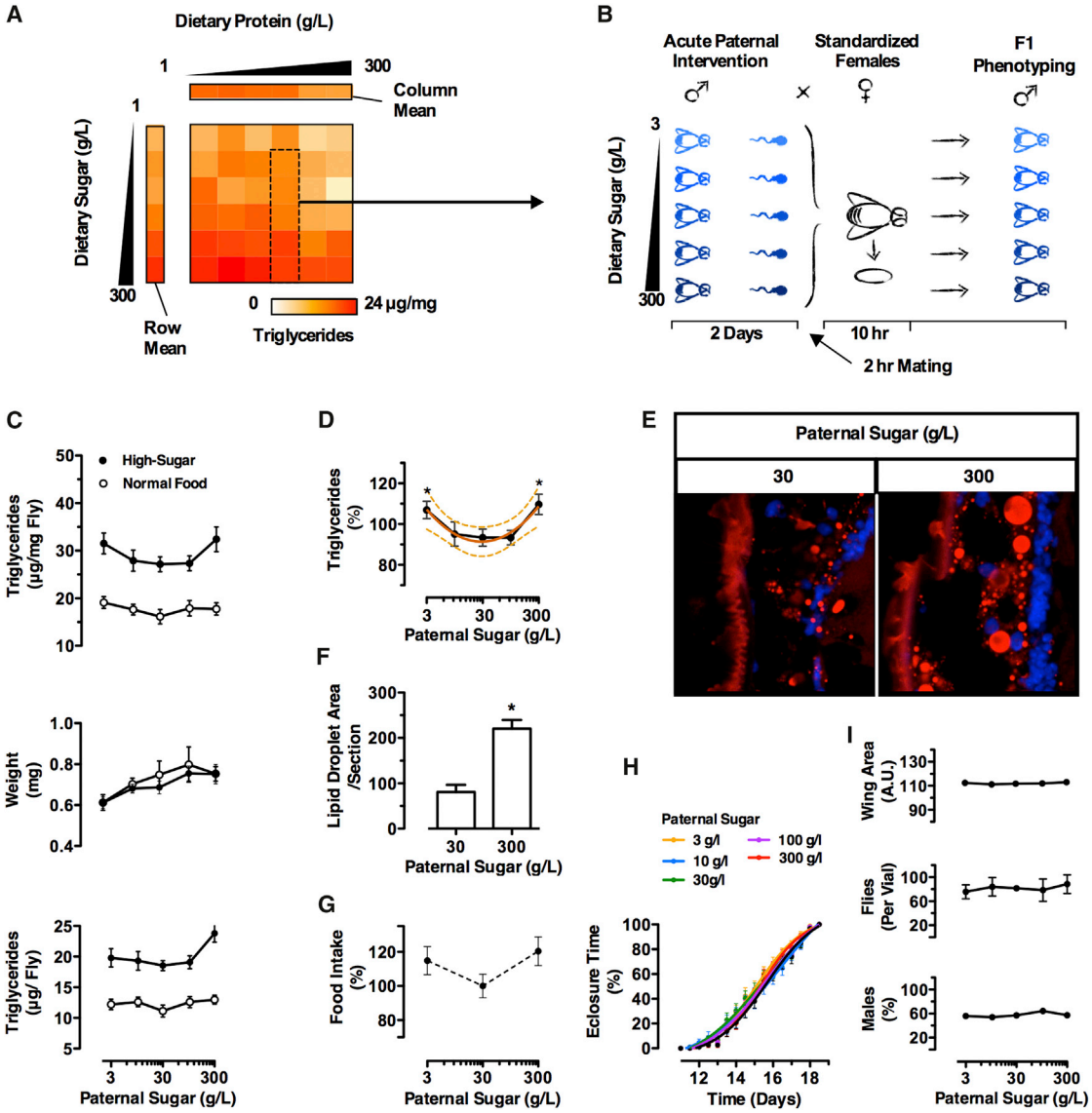

Figure 1. A Fly Model of Paternally Induced Obesity

(A) Triglyceride levels in founder males after 2 days of diet intervention with increasing sugar (sucrose) and protein (soy).

(B) Schematic of the IGMR experimental design.

(C) Triglycerides (top), body weight (middle), and weight normalized triglycerides (bottom) of F1 males raised on normal (open circles) and on high-sugar food (closed circles).

(D) Binomial regression of F1 male weight normalized triglycerides (95% CI, $p < 0.01$).

(E) Representative section of anterior fly fat body stained with oil red O and DAPI.

(F) Lipid droplet area/section.

(G) Food intake of F1 males by CAFE assay.

(H) Ecclosure timing of F1 offspring as percent of total.

(I) (Top) Relative wing area of F1 males. (Middle) Total number of ecclosed offspring per vial. (Bottom) Number of male offspring per vial (% of total flies).

Results are mean ± SEM (*$p < 0.05$) of n = 3–8 experiments each with multiple replicates. See also Figure S1.

PEV in four of the lines tested (A_{480}; Figures 3A–3D), including reporters for telomeric (ChrX; *HA-1902*) (Figure 3A), retrotransposon-type (Chr3R; *HA-1992*) (Figure 3B), pericentric (Chr4;*39c-12*) (Figure 3C), and repeat-associated chromatin (Chr2:3;*92E*) (Figure 3D). Notably, all four lines generated U-shaped paternal IGMR obesity (Figure 3F). Thus, IGMR occurs on independent genetic backgrounds and leaves HA-1902-, HA-1992-, 39c-12-, and 92E-type chromatin largely unaltered.

Intriguingly, when testing w^{m4h}, a reporter for peri-centric heterochromatin on ChrX, we observed a reproducible U-shaped intergenerational eye color phenotype (Figures 3E and 3G). In support of a mechanistic link between the IGMR obesity and

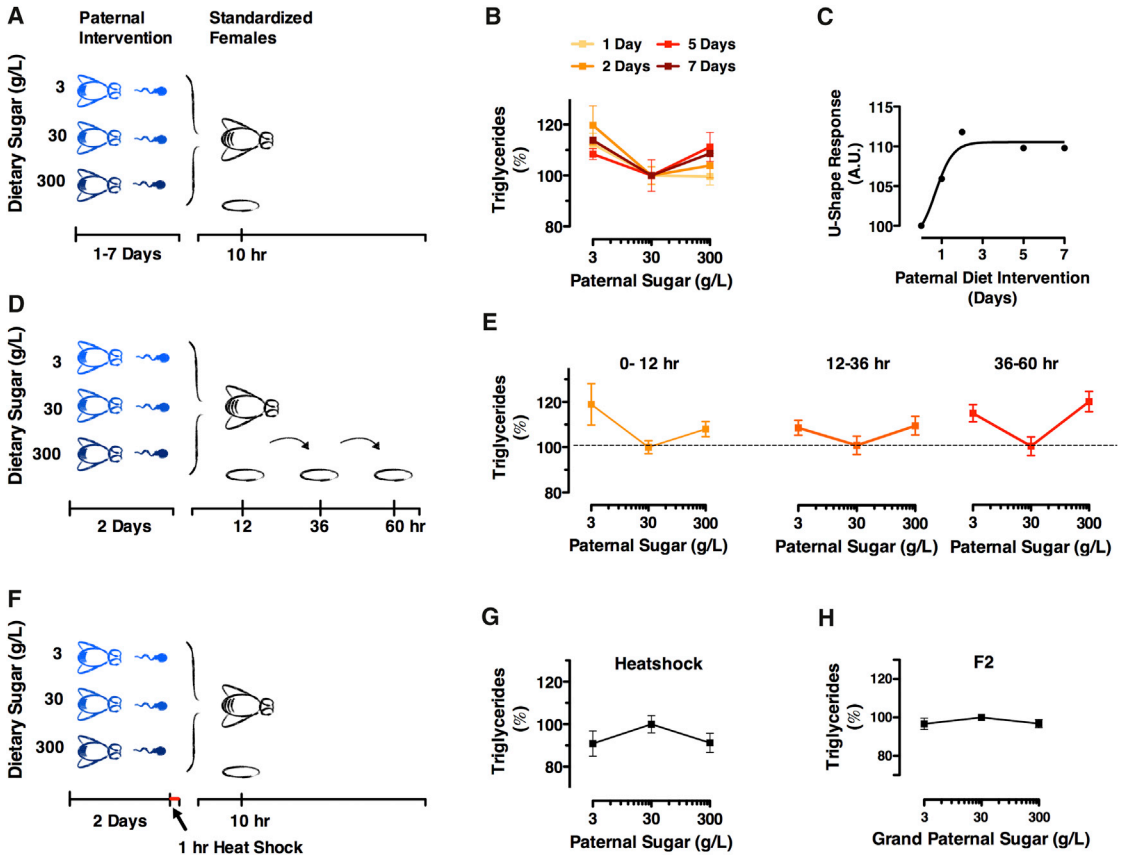

Figure 2. Acute Paternal Nutritional State Is Reflected in Offspring Obesity

(A and B) (A) Schematic and (B) offspring adiposity from tests of progressively increasing paternal dietary intervention.

(C) Mean change in offspring adiposity (Δtriglycerides/weight) for low- and high-sugar-sired adult males relative to medium sugar for each time point. Least square curve fitting (slope = −1, R^2 = 0.95).

(D and E) (D) Schematic and (E) F1 male adult adiposity from tests of consecutive offspring cohorts from the same mating event. After mating, females were kept on standard food, and three consecutive batches of embryos were collected and assessed at adulthood.

(F) and (G) (F) Schematic and (G) offspring adiposity for tests of stress sensitivity. A 1 hr 37 degree heat-shock was applied to males just before mating.

(H) F2 adult male adiposity. F1 males were kept on standard food prior to mating.

Results are mean ± SEM of n = 3–8 experiments each with multiple replicates.

PEV results, triglyceride accumulation and eye color correlated positively; redder-eyed flies were more obese (Figure 3H). No correlation was observed in the remaining four strains (data not shown). These data show that acute paternal diet targets select chromatin subtypes in offspring.

High Paternal Sugar Controls Heterochromatin-Embedded Gene Expression

At this point, we focused on medium- versus high-sugar IGMR and tested whether IGMR affected all or only select individuals in the population. Measuring pigment from single w^{m4h} fly heads as a direct readout of the IGMR response, we observed that paternal IGMR red-shifted the entire distribution (Figures 4A and 4B). Thus, high paternal sugar induces w^{m4h} desilencing population-wide, indicating that each paternal gamete carries an equivalent intergenerational signal.

Next, we performed rRNA-depleted RNA-sequencing of hand-picked stage 17 embryo F1 offspring from medium- and high-sugar challenged fathers (Pearson corr. = 0.97, ~15 million reads/sample; Figure 4C). In support of a selective chromatin state desilencing mechanism, gene expression broadly increased, with many more up- than downregulated transcripts. Sixty-eight protein-coding genes were significantly upregulated in high-sugar sired embryos (mean ΔFPKM = 54.9) and only ten downregulated (mean ΔFPKM = −7.0; Figure 4D and Table S1). Of note, upregulated transcripts tended to be genes highly expressed during late embryo and early larval stages, including 27 (40%) related to biogenesis of the sugar-based cuticle. Of the remaining 42 genes, 30 were of unknown function, 5 had peptidase activity, and interestingly, 4 were metabolic genes, including fatty acyl-CoA reductase and fatty acid elongase.

Analysis using gene set enrichment analysis (GSEA) revealed two clearly upregulated clusters containing *chitin and cuticle constituent* and *mitochondrial and primary energy metabolism* pathways (Figures 4E and S2A and Table S2). Included and consistent with the heightened adiposity of IGMR, pathways

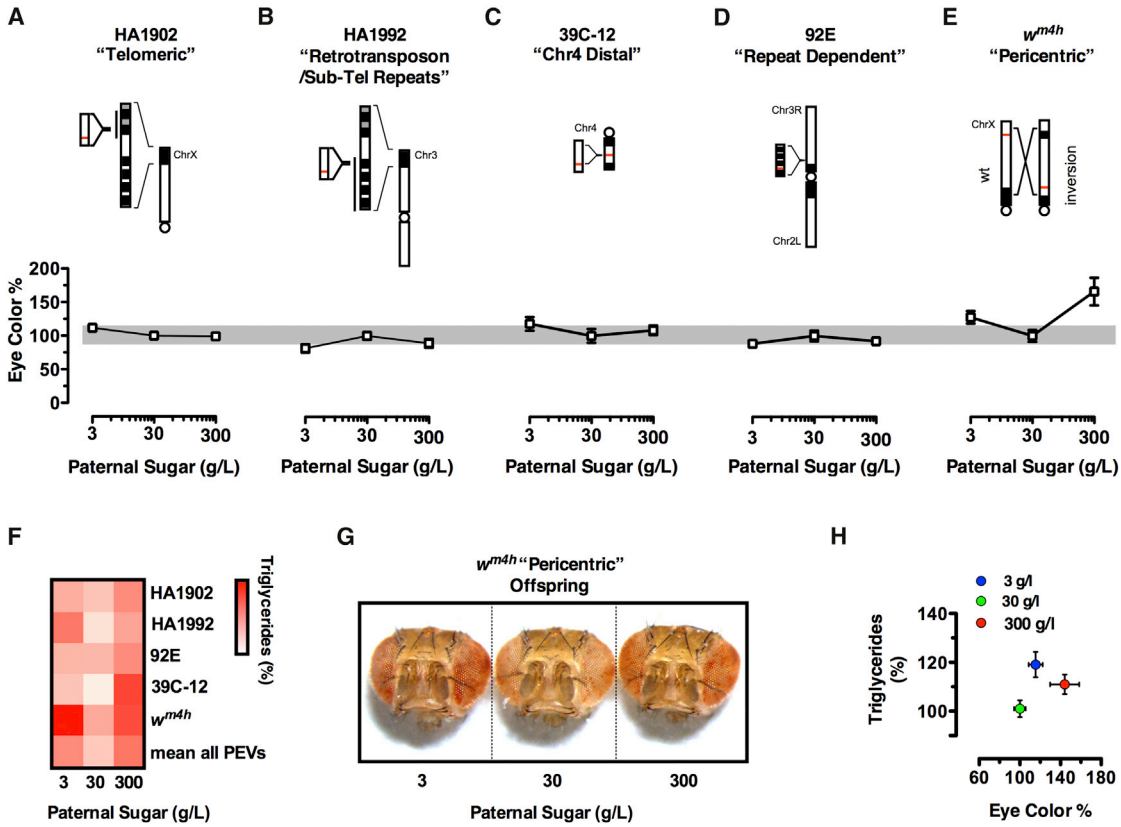

Figure 3. High Paternal Sugar Is a Physiological Su(var)

(A–E) (Top) Schematics of (A) *pP{RS5}5-HA-1902*, (B) *pP{RS5}5-HA-1992*, (C) *39C-12*, (D) *T(2;3)V21ePlacW* (*92E*), (E) *In(1)*w^{m4h} PEV reporters. (Bottom) Eye pigment absorption (A_{480}) from heads of adult males, normalized to offspring of paternal 30 g/l sugar.

(F) Heatmap of paternal IGMR offspring from the PEV lines in (A–E). Triglyceride/weight normalized to paternal 30 g/l sugar.

(G) Representative median eye-colored w^{m4h} fly heads from 3, 30, and 300 g/l sugar-sired offspring.

(H) Correlation of eye color (heads) and offspring triglyceride/weight (carcass rest) of w^{m4h} flies measured in the same individuals.

Results are mean ± SEM of n = 3–8 experiments each with multiple replicates.

for *lipid particle*, the electron transport chain complexes I, IV, and V, *glycolysis*, *TCA cycle*, and *fatty acid metabolism* were all upregulated. These changes are consistent with energetics of enhanced lipid storage (Figure S2B). Three downregulated clusters were also detected, including *cell cycle and mitosis*, *body patterning*, and intriguingly, a cluster of *chromatin regulation* pathways. Consistent with sensitivity of the pericentric w^{m4h} reporter to IGMR *chromosome*, "*centromeric region*" was ranked second in the chromatin cluster and "*chromatin silencing*" ranked third. Examination of genes annotated as PEV suppressing, also known as *Su(var)'s*, revealed a concerted ~10%–20% downregulation, including members of most well-documented silencing pathways (Figure S2C and Tables S2 and S3). Thus, the IGMR embryo is characterized by gene expression favoring primary energy metabolism over chromatin control.

We next compared our data with chromatin mapping data sets from the community. Filion et al. used Dam-ID to annotate five major chromatin types, three repressive (black, blue, and green) and two active (red and yellow) (Filion et al., 2010). When intersecting our IGMR embryo data with their chromatin state maps, strong enrichment was observed in high-sugar sired embryos for genes embedded in "black" lamin/H1-associated heterochromatin and "blue" polycomb-associated chromatin, and relative depletion was observed for those annotated as "yellow," or housekeeping-type chromatin (Figures 4F and 4G). These findings were verified using rank-order (Figure 4F) and differential expression analyses (Figure 4G). No global effect was observed on "red" or "green" chromatin embedded genes. Consistent with these global indications of chromatin state dependency, the 68 significantly upregulated genes were almost exclusively found in "black" or "blue" chromatin while the 10 significantly downregulated transcripts were randomly distributed (Figure 4H). These data identify high paternal sugar as a chromatin-state-selective physiological Su(var) and identify IGMR as chromatin state dependent.

Polycomb and Core Heterochromatin Machinery Mediate Paternal IGMR

To genetically validate chromatin state regulation as a mechanistic underpinning of our model, we began systematically testing IGMR potential in mutants known to modify w^{m4h} variegation. We started with *Su(var)3-9*^{06}, a homozygous dominant suppressor allele of the H3K9 histone methyltransferase Su(var)3-9.

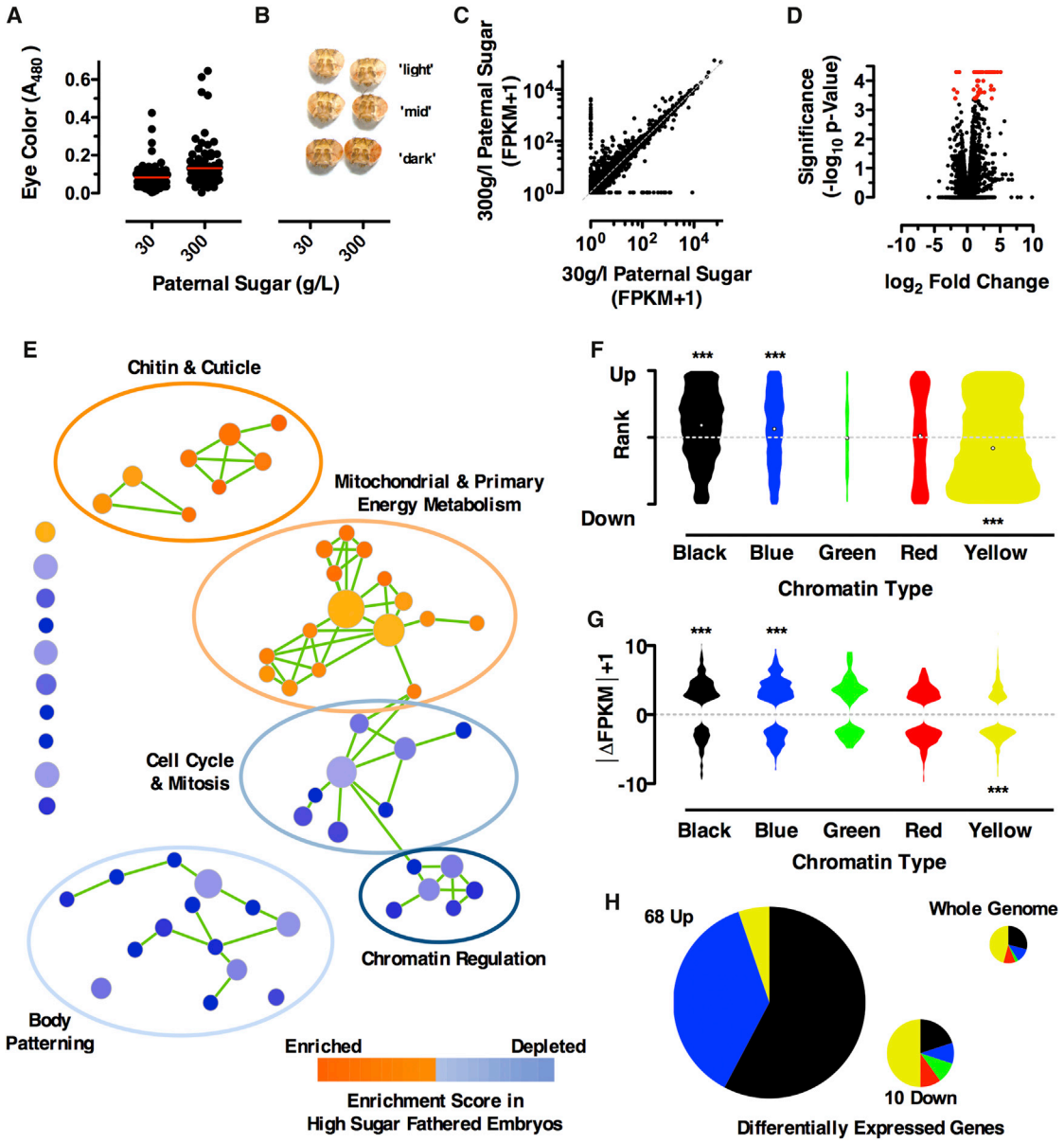

Figure 4. Paternal IGMR Alters Select Chromatin States in Offspring

(A) Interindividual variation of eye color of w^{m4h} flies from fathers fed high (300 g/l) or medium (30 g/l) sugar food.

(B) Representative heads from w^{m4h} offspring. Shown are heads representative of light, medium, and dark red eyes of each respective cohort.

(C–H) RNA-sequencing results of medium (30 g/l) and high-sugar (300 g/l) sired stage 17 embryos. (C) FPKM plot. (D) Volcano plot.

(E) Cytoscape enrichment map (p cutoff: 0.005, FDR Q-value cutoff: 0.025, overlap cutoff: 0.2) of gene set enrichment analysis (GSEA). (Orange) Gene sets enriched; (blue) gene sets depleted, in high-sugar IGMR. Color intensity reflects degree of enrichment. Major clusters are circled.

(F and G) (F) Rank and (G) absolute IGMR expression changes. Genes are allocated to one of five chromatin states (colors) according to their TSS (Filion et al., 2010). Plotted are (F) ranks for all genes and (G) absolute expression changes of the top 1,000 IGMR up and downregulated genes.

(H) Chromatin color annotation of all significantly up- and downregulated IGMR genes.

See also Figure S2.

Medium- and high-sugar-challenged *Su(var)3-9*^{06} fathers were mated with standardized w^{1118} females, and the resulting heterozygote offspring were monitored for adiposity (Figure 5A). Whereas w^{1118} animals reproducibly exhibited a ~10%–15% increase in adiposity upon high-sugar IGMR, F1 adult male offspring of *Su(var)3-9*^{06} fathers showed no intergenerational obesity response (Figure 5A). This provides genetic evidence that Su(var)3-9 is required for IGMR.

We also tested a second H3K9 methyltransferase, SetDB1. As heterozygotes, *SetDB1*^{1473} fathers gave both wild-type and mutant offspring. Intriguingly, both mutant (Figure 5B, red) and wild-type *SetDB1*^{1473} fathered offspring (Figure 5B, black)

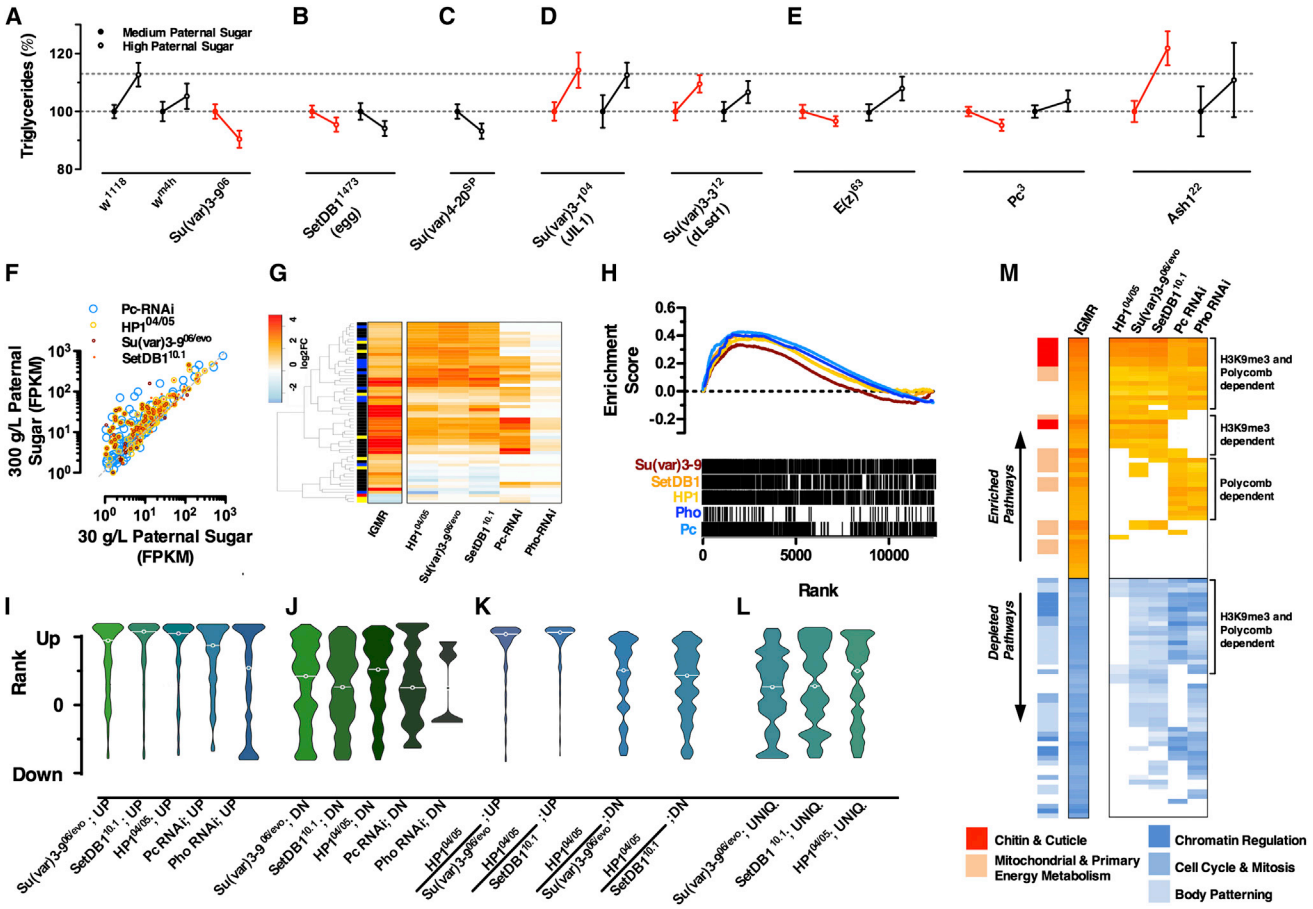

Figure 5. A Su(var)/PcG Axis Essential for Paternal IGMR

(A–E) Adiposity of offspring (triglycerides/weight) of mutant fathers challenged with medium (30 g/l; closed circles) or high sugar (300 g/l; open circles). Gray dashed line indicates normal w^{1118} IGMR response. IGMR adiposity responses are shown for offspring of (A) w^{1118}, w^{m4h}, and *Su(var)3-9*^{06}, (B) *SetDB1*^{1473}, (C) *Su(var)4-20*^{SP}, (D) *Su(var)3-1*^{04}, *Su(var)3-3*^{12}, (E) *E(z)*^{63}, *Pc*^{3}, and *Ash1*^{22} mutant (red) and wild-type (black) offspring. Results are mean ± SEM of n = 3–8 experiments each with multiple replicates.

(F) FPKM values of RNaseq data from medium and high-sugar-fathered embryos. 200 most upregulated genes from HP1 (open yellow), *Su(var)3-9* (closed cayenne), and *SetDB1* (closed orange) mutant first-instar larvae from Lundberg et al. (2013) and Pc-RNAi (open blue) experiment from Goodliffe et al (2007).

(G) Heatmap of expression changes of significantly changed genes in our paternal IGMR offspring embryo data set and in the Lundberg et al. *HP1*, *Su(var)3-9*, and *SetDB1* mutants and the Goodliffe et al (2007) *Pc*-, *Pho*-RNAi data sets.

(H) Enrichment plot for gene sets upregulated in *HP1*$^{04/05}$ (yellow), *Su(var)3-9*$^{06/evo}$ (cayenne), and *SetDB1*$^{10.1}$ (orange) mutants and *Pc*- (light blue) and *Pho*-RNAi (dark blue) in our stage 17 paternal IGMR offspring embryos.

(I–L) Violin plots of expression change distributions relative to all genes of stage 17 paternal IGMR offspring embryos for gene sets from *HP1*$^{04/05}$, *Su(var)3-9*$^{06/evo}$, and *SetDB1*$^{10.1}$ mutants (Lundberg et al.) and from *Pc* and *Pho*-RNAi embryos (Goodliffe et al.). IGMR relative rank is plotted for all available of the (I) 200 genes most upregulated and (J) 200 genes most downregulated by each mutant / RNAi line; (K) intersects of the 200 most up- or downregulated genes of the indicated pairs of mutants; and (L) genes in the 200 most upregulated gene sets unique to each respective mutant.

(M) Heatmap comparison of GSEA results from mutant and IGMR data. Plotted are the 50 most up- and downregulated pathways from paternal IGMR and respective scores from the mutant data sets. Colored bars left of the heatmap indicate clusters in Figure 4E.

completely failed to mount an IGMR obesity response (Figure 5B). *Drosophila* sperm develop as a syncytium, and therefore both mutant and wild-type sperm in such a cross will share a *SetDB1*^{1473} mutant cytosolic compartment for most of their development. These findings therefore indicate that SetDB1 in the male germline is necessary for proper IGMR.

H4K20me3 deposition follows H3K9me3 in the establishment of heterochromatin (Schotta et al., 2004). We therefore also tested *Su(var)4-20*^{SP}, a mutant for the H4K20 methyltransferase Su(var)4-20. As *Su(var)4-20*^{SP} is on Chr X, all male offspring from our crosses are wild-type. Again though, wild-type offspring will reflect the mutant heterozygosity of spermatogenesis. *Su(var)4-20*^{SP} fathers failed to transmit paternal IGMR to the F1 (Figure 5C). Thus, uncompromised expression of *Su(var)3-9, SetDB1*, and *Su(var)4-20* are absolutely required for IGMR. Of note, not all w^{m4h} suppressor alleles were IGMR incompetent. *Su(var)3-1*^{04} and *Su(var)3-3*^{12}, also known as Jil1 kinase and dLSD1, respectively, generated completely normal IGMR obesity responses (Figure 5D), thus indicating that IGMR is not directly linked to the w^{m4h} insertion locus itself. These findings

identify one of the first gene networks known to be absolutely required for proper intergenerational metabolic reprogramming.

Given the observed derepression in blue embedded genes (polycomb-associated; Figure 4), we tested IGMR potential in polycomb and trithorax group mutants. We found that, although *Ash1*^{22} mutants were fully IGMR competent, *Enhancer of zeste*, *E(z)*^{63} and *Polycomb*, *Pc*^{3} mutant males completely failed to elicit a response in the next generation (Figure 5E). Thus, polycomb- and H3K9me3-centric chromatin regulators are absolutely required for paternal diet-induced intergenerational obesity.

The IGMR Program Is Chromatin Encoded

To corroborate these findings, we compared our embryonic IGMR RNA-seq data with profiles from H3K9me3- and polycomb-insufficient mutants. We examined profiles from *Su(var)3-9*$^{06/evo}$, *SetDB1*$^{10.1}$, and *HP1*$^{04/05}$ mutant first-instar larvae (Lundberg et al., 2013) and *Pc*- and *Pho*-RNAi knockdown embryos (Goodliffe et al., 2007). Intriguingly, ~70% overlap was observed between our significantly dysregulated IGMR genes and those responsive to H3K9-centric or polycomb insufficiency (Figures 5F and 5G). The converse was equally true; each of the top 200 *Su(var)3-9*$^{06/evo}$, *SetDB1*$^{10.1}$, *HP1*$^{04/05}$, *Pho-RNAi*, and *Pc-RNAi* dysregulated gene sets showed strong enrichment in our high-sugar-sired F1 embryos (Figure 5H). Subgrouping confirmed specificity of these signals. First, transcripts upregulated by *Su(var)3-9*$^{06/evo}$, *SetDB1*$^{10.1}$, *HP1*$^{04/05}$, *Pho*, and *Pc* insufficiency (likely direct targets) showed clear coordinate increases in expression (Figure 5I) compared to apparently randomly distributed signals for transcripts downregulated by mutation (Figure 5J). Transcripts upregulated by both *HP1*$^{04/05}$ and either *Su(var)3-9*$^{06/evo}$ or *SetDB1*$^{10.1}$ (Figure 5K) showed much stronger signatures than transcripts significantly regulated by any one Su(var) mutant alone (Figure 5L). Thus, paternal IGMR mimics H3K9me3- and polycomb-dependent transcriptional dysregulation.

To test whether these signatures might directly contribute to metabolic reprogramming, we performed GSEA analysis of the Lundberg et al. (2013) and Goodliffe et al. (2007) data sets. Coordinate overlapping enrichment signatures were observed for key pathways of all five major IGMR clusters (Figure 5M and Table S2), including most chromatin and primary energy modules. Of note, the most significantly enriched pathways in our data set were those regulated by both silencing systems together (Figure 5M). Thus, IGMR is characterized by H3K9me3-/PcG-dependent dysregulation.

Sperm and Zygote Chromatin Plasticity Define IGMR

To gain further insight into IGMR transmission, we performed RNA sequencing from manually dissected and purified mature sperm of high- and medium-sugar-fed *w*^{1118} males (Table S4). Intriguingly, we again observed clear evidence of (1) broad transcriptional derepression in sperm of high-sugar-fed males (Figures 6A and 6B), (2) selective upregulation of black chromatin-embedded genes (Figure 6C), and (3) upregulation of *Su(var)3-9*$^{06/evo}$-sensitive genes (Figure 6D). These data indicate that transcriptional dysregulation in mature IGMR sperm is also chromatin state defined. In contrast to the embryo data, blue and yellow embedded genes appeared largely unaffected in the sperm transcriptome. Thus, chromatin-dependent signatures of IGMR are forecast in the P0 paternal germline.

Dysregulation of black embedded genes in both the sperm and zygote suggested potentially overlapping mechanisms for generation of the intergenerational signal in the germline and for hardwiring the IGMR phenotype in the offspring. To probe this idea genetically, we compared the effect of maternal versus paternal mutant allele contribution on IGMR. As described above, offspring of Su(var) and Polycomb mutant fathers were incapable of mounting an IGMR response (Figures 5A–5E and 6E, top row). In crosses in which *Su(var)3-9*$^{06/evo}$, *SetDB1*$^{10.1}$, or *Su(var)4-20*^{SP} mutations were contributed by the oocyte, IGMR-competent wild-type sperm were no longer able to evoke an intergenerational response (Figure 6E, bottom row). *Su(var)3-1*^{04} and *Su(var)3-3*^{12} mutants, unremarkable in the male germline, completely abrogated the response when contributed maternally (Figure 6E, bottom row). In contrast, oocytes contributing *Pc*^{3} and *E(z)*^{63} mutations, whose constitutive heterochromatin would not be predicted to be directly perturbed, mounted completely normal IGMR responses. Collectively, these data support a model in which IGMR results from and requires a permissive range of heterochromatin plasticity in the zygote.

To validate the idea, we intersected our embryo RNA-seq data with modENCODE H3K9me3 and H3K27me3 ChIP-seq profiles from same-stage embryos (16–20 hr) and from those isolated one time point earlier in development (12–16 hr), enabling us to gauge the dynamics of K9me3/K27me3 gain and loss (Nègre et al., 2011). We made several observations. First, IGMR-dysregulated genes represented a class undergoing highly dynamic H3K9 and H3K27 trimethylation (Figure 6F). This was true for our significantly changed IGMR genes, as well as the leading edge H3K9me3- and polycomb-dependent IGMR gene sets from Figure 5I (Figure 6F and data not shown). The bodies of these genes in particular were unmarked in 12–16 hr embryos and exhibit strong H3K9me3 and H3K27me3 just 4 hr later. Importantly, we observed the same signature when analyzing leading-edge genes of metabolic pathways upregulated in our obese IGMR phenotype (Figure S3A). Thus, genes undergoing highly dynamic H3K9me3- and H3K27me3-dependent silencing are specifically targeted for IGMR derepression.

Because repressive marks correlate with the higher-order chromatin structure and *cis*-regulatory domain organization, we also examined our gene sets in the context of insulator occupancy (Nègre et al., 2010). Analysis revealed that all three IGMR-dysregulated gene sets were on average far from class I (*CTCF*, *CP190*, and *BEAF*-associated) and were somewhat closer to class II (*SuHw*-associated) insulators (Figure 6G). These signatures were specific when compared to similarly expressed genes or to the entire transcriptome (Figure 6H, left). Intriguingly, the same signature was again evident in our most up- and downregulated sperm transcripts (Figure 6H, right). Thus, IGMR impacts spatially and chromatin-context-defined transcriptional units in fathers and in offspring.

Collectively, our data suggest that IGMR results from global alterations in chromatin state integrity within a permissive window, where obesity susceptibility results from reduced stage-specific epigenetic regulation of H3K27me3- and H3K9me3-defined domains. Our observations of *w*^{m4h} eye color desilencing (Figures 3

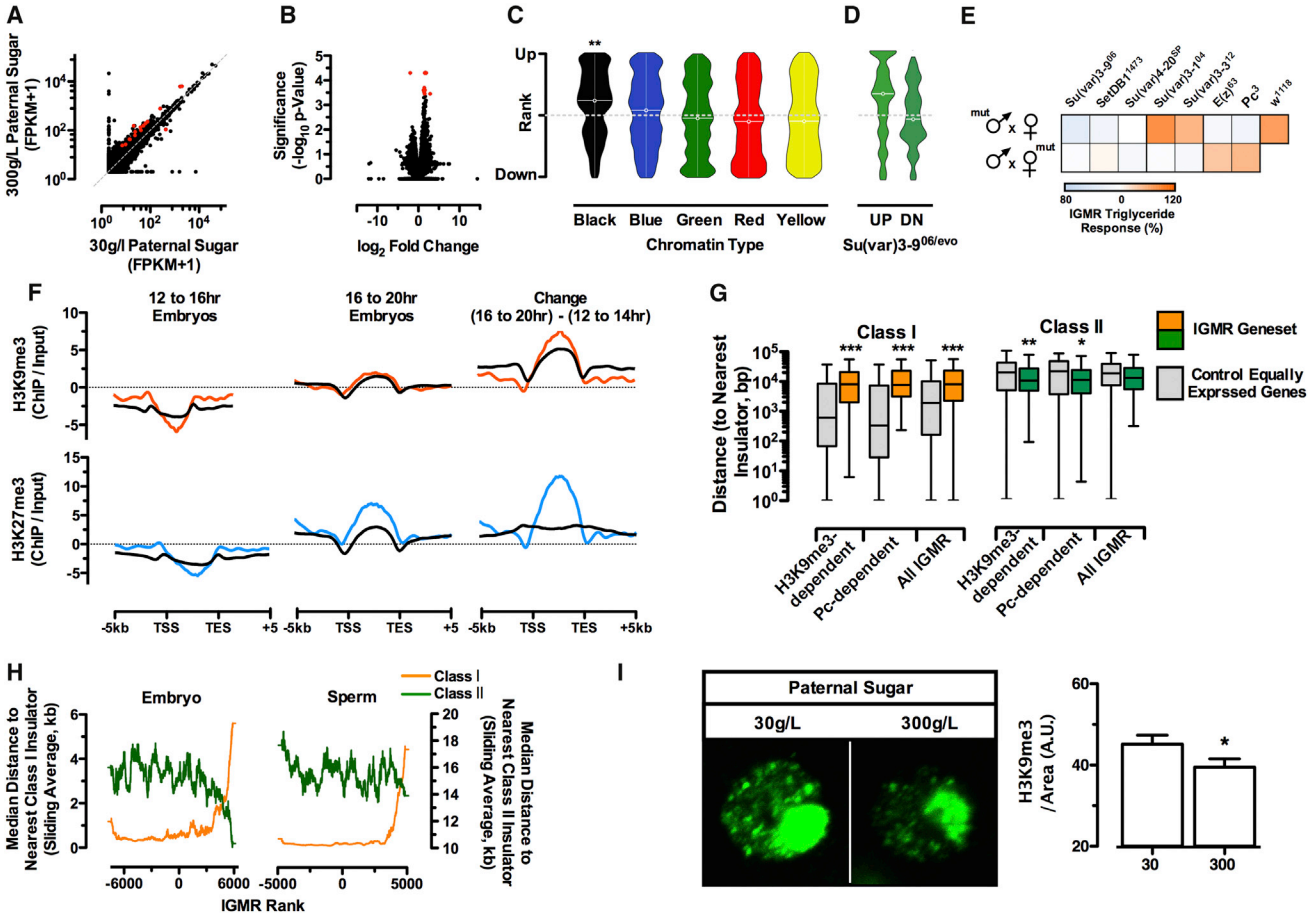

Figure 6. IGMR Signatures Are Forecast in the P0 Germline, and IGMR Changed Genes Show K9/K27me3 Dynamic Context

(A–D) RNA-sequencing results of sperm from medium- (30 g/l) and high-sugar (300 g/l) fed fathers; significantly changed genes are depicted in red. (A) FPKM plot. (B) Volcano plot. (C and D) IGMR expression changes in sperm of high- relative to medium-sugar-fed fathers (C) for the five chromatin colors according to Filion et al. (2010) and (D) for 200 most up- or downregulated genes from *Su(var)3-9*$^{06/evo}$ mutants from Lundberg et al (2013).

(E) Relative adiposity of male offspring (triglycerides/weight) (top row) from crosses of mutant fathers challenged with medium- or high-sugar diet, with w^{1118} mothers and (bottom row) of crosses of w^{1118} fathers with mutant mothers. The normal w^{1118} IGMR response is also shown (top row). Results are mean ± SEM of n = 3–8 experiments each with multiple replicates.

(F) ChIP/input signal from modENCODE data sets for leading-edge H3K9me3- and polycomb-dependent genes (red in top panels, blue in bottom panels) in our IGMR offspring embryo RNA-seq. H3K9me3 (top) and H3K27me3 (bottom) enrichment of 12- to 16-hr-old and 16- to 20-hr-old embryos (left) and the difference between the two stages (right). Black lines present the average for all genes.

(G) Box plots of distance to nearest class I and class II insulators. Shown are distances for leading-edge *Su(var)* and *PcG* upregulated genes in our IGMR offspring embryo RNA-seq. Grey boxes represent a control set of equally expressed genes. The boxes indicate the first and third quartiles, and the central line indicates the median. Whiskers extend to the most extreme data point, which is no more than 1.5 times the quartile range.

(H) Distance to nearest class I (orange) and class II (green) insulator plotted according to ranked expression change from IGMR RNA-seq results (high versus medium sugar). Values are sliding window averages of 500 genes.

(I) (Left) H3K9me3 staining of fat body cell nuclei from offspring of medium (30 g/l) and high-sugar (300 g/l) fed fathers. Results are mean ±SEM of n = 7 experiments, each with multiple replicates. (Right) Quantification of fat body cell nucleus H3K9me3 staining.

See also Figure S3.

and 4) and reductions in H3K9me3 immunofluorescence in adult IGMR offspring fat bodies (Figure 6I and Figure S3B) indicate that this chromatin state reprogramming is stable lifelong in the offspring.

A Conserved Signature for Chromatin-State-Associated Phenotypic Variation

More fundamentally, the above data identify a mechanism that directionally controls phenotypic variation within a population. To probe potential conservation of such processes, we searched for similar signatures in data sets from mouse and man. We examined two murine and three human microarray data sets focusing on adipose tissue from lean and obese individuals, first defining mouse and human ortholog pathways to all Flybase-annotated *Drosophila* Su(var)'s and then by using GSEA to test for dysregulation (Figures 7A–7D). Intriguingly, we observed clear signatures of Su(var) depletion in obese individuals in two of the most highly genetically controlled human adiposity data

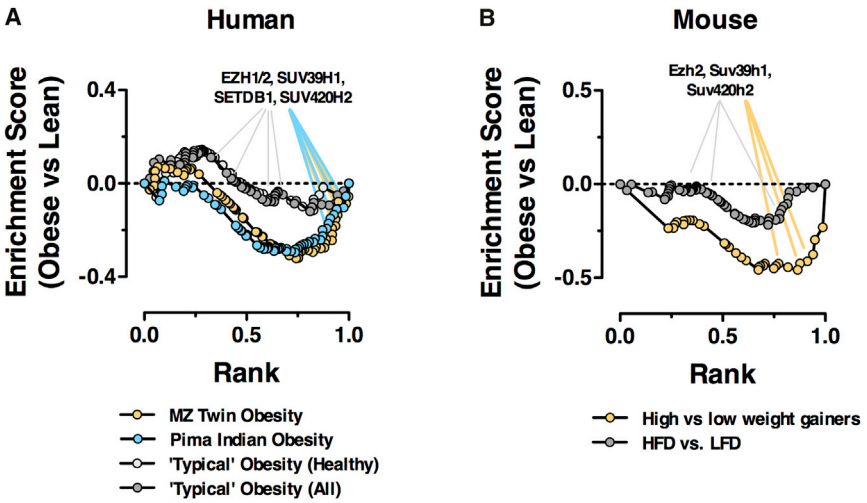

Figure 7. An IGMR Signature Conserved from Fly to Man

GSEA of mouse and human ortholog pathways for all Flybase-annotated *Drosophila* Su(var)'s (A) in three human adiposity data sets: 19 obese versus 20 non-obese Pima Indians by Lee et al. (2005); 13 human monozygotic (MZ) twin pairs, each discordant for obesity by Pietiläinen et al. (2008); and a human cohort for "typical" obesity by Klimcáková et al. (2011) and (B) in two murine obesity samples: surgically isolated adipose tissue of future high and low weight gainers from C57BL6/J mice biopsied prior to treatment with high-fat diet by Kozak et al. and diet-induced obesity comparing high- versus low-fat-diet-treated C57BL6/J animals by Voigt et al (2013).

sets available: first in a study of 19 obese versus 20 non-obese Pima Indians (Lee et al., 2005) and then, even more compelling, in a collection of 13 monozygotic twin pairs, each with one normal and one obese co-twin (Pietiläinen et al., 2008) (Figure 7A). Examination of the first figure in the latter study reveals clear evidence also of transcriptome-wide desilencing, with ~5-fold more up- versus downregulated genes in the obese co-twins. Further, similar signatures appear to predict murine obesity susceptibility. In an elegant study, Koza et al. isolated adipose tissue from young C57BL6/J mice prior to treatment with high-fat diet (Koza et al., 2006). Profiling the pretreatment samples from the lowest and highest weight gainers of the 107 animal strong cohort, the authors were able to establish predictive signatures for obesity susceptibility. Reanalyzing these data, we found clear evidence that Su(var) pathway depletion predicts obesity susceptibility (Figure 7B).

Leading-edge analysis of all three data sets revealed orthologs of our IGMR defining Su(var)3-9, Setdb1, Su(var)4-20, and E(z) regulators as driving the GSEA signal (Figures 7A and 7B, highlighted genes). Importantly, no obvious signatures were observed in an independent "typical" human obesity cohort in which the obesity is most likely driven by assorted genetic factors (Figure 7A) (Klimcáková et al., 2011), nor were they observed in diet-induced obese C57BL6/J mice (Figure 7B) (Voigt et al., 2013). Thus, Su(var) suppression characterizes obesity susceptibility on defined human and mouse genetic backgrounds.

These data identify conserved gene signatures for epigenetically defined phenotypic variation from fly to mouse to man.

DISCUSSION

Intergenerational Control of Chromatin State and Obesity

Here, we show that acute dietary interventions, as short as 24 hr, have the capacity to modify F1 offspring phenotype via the male germline. We show that reprogramming occurs in response to dietary manipulations over a physiological range and that phenotypic outcomes require polycomb- and H3K9me3-centric plasticity in spatially and chromatin-state-defined regions of the genome. The eye color shifts in w^{m4h} offspring (Figures 2E, 2G, and 2H) and the reduced fat body H3K9me3 staining in adult IGMR offspring (Figure 6I) supports the conclusions, first, that there are chromatin state changes and, second, that these are stable lifelong. These data are corroborated by selective derepression of *Su(var)3-9*, *SETBD1*, *Su(var)4-20*, and polycomb-sensitive transcripts (Figures 5F–5M); chromatin-state-associated transcriptional rearrangements genome wide (Figures 4F and 6C); selective reprogramming of highly dynamic histone-mark-defined regions (Figure 6F); and the fact that IGMR itself is sensitive to a string of distinct H3K9me3-centric and polycomb mutants (Figures 5A–5E). Although nontrivial, ChIP-seq comparisons of repressive chromatin architecture in mature sperm and multiple defined offspring tissues will be important to establishing the ubiquitousness of these regulatory events and the nature of intergenerational signal itself. These data highlight how acutely sensitive intergenerational control can be to even normal physiological changes, and they identify some of the first genes absolutely required for transmission.

Paternal Diet Regulates Chromatin-Defined Genes in the Germline and Offspring

First categorized simply as heterochromatin versus euchromatin, multiple empirical models now divide the genome into 5 to 51 chromatin states, depending on the analysis (Filion et al., 2010; Kharchenko et al., 2011; Ernst and Kellis, 2010). We find that paternal high sugar increases gene expression preferentially of heterochromatic-embedded genes in embryos. Specifically, these genes are characterized by active deposition of H3K9me3 and H3K27me3, by long distance from class I insulators, and by sensitivity to fully intact expression of *Su(var)3-9*, *Su(var)4-20*, *SetDB1*, *Pc*, and *E(z)*. The data support a model where phenotype has been evolutionarily encoded directly into the chromatin state of relevant loci. Specifically, an abundance of genes important to both cytosolic and mitochondrial metabolism appear to be embedded into H3K9me3- and distinct polycomb-dependent control regions. Indeed, our own GO analysis of the five chromatin colors from Filion et. al. (2010) indicate a largely mutually exclusive picture, in which functional pathways

are not randomly distributed across chromatin states (data not shown). Our paternal IGMR data set revealed clear and strong overlaps with pathways of black (lamin-associated) and blue (polycomb) chromatin and included many key metabolic pathways, including *glycolysis*, *TCA cycle*, mitochondrial OxPhos, *chitin*, and *polysaccharide metabolism*, changes that could well prime the system for altered functionality given the appropriate stimulus. Indeed, our paternal IGMR phenotype is a susceptibility to diet-induced obesity and is most readily observable upon high-sugar diet challenge.

Chromatin state coding of functional gene sets would provide a simple mechanism for transgenerational environmental response capable of rewiring even the earliest events of zygotic genome activation. The idea is also consistent with parallel avenues of research already in the literature. rRNA genes, for instance, are not only sensitive to the same Su(var)'s but are also known to influence metabolic gene expression and growth (Paredes et al., 2011). Flies with fewer rRNA genes (rDNA) exhibit a phenotype called bobbed (bb), which results in smaller bristles, a reduced growth rate, and a thinner chitinous cuticle (Ritossa et al., 1966). These phenotypes are intriguingly similar to the top GSEA enrichment clusters that we observed for IGMR, namely cell cycle, body morphogenesis, chitin deposition, and metabolism. Interestingly, the very same pathways (chitin synthesis, TCA cycle, carbohydrate, and lipid metabolism) are regulated by nutritional status in third-instar larva (Teleman et al., 2008), suggesting that the paternal IGMR signal acts to prime offspring for metabolic challenge.

Our data support a *trans*-acting mechanism. In the w^{m4h} experiments, male offspring inherited their X chromosome and thus the reporter from their unchallenged mothers, i.e., the reporter allele never encounters the initial signal but is reproducibly reprogrammed. Further, the failure of $Su(var)4\text{-}20^{SP}$ and $SetDB1^{1473}$ mutants to elicit IGMR responses in their wild-type offspring indicate that wild-type haploid sperm carry the same insufficient reprogramming template as their syncytial mutant counterparts. *cis*- and *trans*-acting mechanisms are not mutually exclusive though. Signals transmitted via paternal chromosomes, though likely transmitted in *cis*, may be manifest via expression of paternal transcripts, which then act in *trans*. Paternal reductions of Su(var)3-9, SetDB1, and Hp1, for instance, would affect the maternal genome in *trans*.

One Genotype, Multiple Paternally Directed Phenotypes

Despite their genetic similarity, isogenic or congenic animals reared under controlled conditions exhibit measurable variation in essentially all phenotypes. Such variability in genome output is thought to arise largely from probabilistic or chance developmental events in early life (Burga et al., 2011) (review in Whitelaw et al., 2010). Here, we map a mechanism that couples acute paternal feeding and zygotic chromatin state integrity directly to phenotypic output of the next generation. We find that these same signatures predict obesity susceptibility in isogenic mouse and human obesity cohorts. Because acute circadian fluctuations in feeding are essentially constant over evolutionary timescales, they are the perfect mechanistic input upon which a system could evolve to *ensure* defined phenotypic variation within a given population.

EXPERIMENTAL PROCEDURES

Fly Husbandry

Fly stocks were maintained on standard diet at 25°C on a 2 week generation cycle, ensuring a constant ancestral larva density. w^{1118} flies were single-sibling inbred for ten generations and maintained at a fixed fly density for another ten generations before experimental start. Fly strains used: ln(1)w^{m4h} (w^{m4h}), *pP{RS5}5-HA-1902* (*HA-1902*), *pP{RS5}5-HA-1992* (*HA-1992*), and *pP{RS5}5-HA-1925* (*HA-1925*) and *T(2;3)V21ePlacW* (*92E*), $Su(var)3\text{-}9^{06}$, $Su(var)2\text{-}5^{05}$, $Su(var)3\text{-}1^{04}$, $SetDB1^{1473}$, $Su(var)3\text{-}3^{12}$ from (Phalke et al., 2009). *39C-12* from Sarah Elgin, Pc^{3} and $E(z)^{63}$ from Leonie Ringrose. PEV lines were single-sibling inbred for ten generations.

Standard diet: Agar 12 g/l, yeast 18 g/l, soy flour 10 g/l, yellow cornmeal 80 g/l, molasses 22 g/l, malt extract 80 g/l, Nipagin 24 g/l, propionic acid 6,25 ml/l. Paternal diet intervention: Agar 12 g/l, yeast 10 g/l, propionic acid 4,5 ml/l, soy flour 30 g/l and white sugar as indicated.

Phenotyping

Body weight of five 7- to 12-day-old males flies was measured on a microbalance. Wing area determinations were made using ImageJ. Triglycerides (GPO Trinder, Sigma) and glucose and trehalose (Sigma; GAGO-20) were measured on centrifuged cleared lysates from groups of five flies crushed and sonicated in 100 µl RIPA buffer or TB buffer with or without trehalase (Sigma; T8778-1UN). "Café" assay was performed according to standard procedures. CO_2 production was quantified using a modification of Kucherenko et al. (2011). Eye pigment (A_{480}) was measured in centrifuge-cleared sonicates of one or five fly heads in 20/100 µl RIPA buffer, respectively. Fat body cryosections were fixed for 10 min in 2% formaldehyde in PBS, washed four times for 5 min each in PBS followed by immunofluorescence staining using rabbit anti-H3K9me3 (1:1000, upstate 07-442) and anti-Rabbit Alexa Fluor 488 (1:500; Molecular Probes). Confocal microscopy (LSM 700, Zeiss) analysis used Volocity 5.5 software (Perkin Elmer).

Sperm Dissection

Sperm dissection was modified from Dorus et al. (2006). See additional details in Extended Experimental Prodedures.

RNA Seqencing

Trizol-purified RNA was treated with Ribo-Zero (Epicenter) and libraries prepared with a TruSeq stranded kit (Illumina). > 15 million reads per sample were mapped using TopHat v2.0.8, with -G option against the *Drosophila melanogaster* genome (assembly BDGP5, Ensembl release 69). Gene expression values and significantly differentially expressed genes were calculated using Cuffdiff v2.1.1 with upper-quartile normalization and weighting multimapping reads (-N -u options).

Bioinformatic Analysis

Gene set enrichment analysis used GSEA 2.0 or GSEAPreranked with default parameters. Enrichment plots used the Cytoscape plugin Enrichment Map. Analysis of the five chromatin colors used BedTools (2.16.2). For microarray analyses, normalized probe values from the authors were mapped using Ensembl Biomart, and differential analysis against corresponding wild-types were performed using limma in R. Statistically significant was adjusted p value < 0.05 and fold change > 2. Enrichment of chromatin and insulator ChIP-seq data sets from modENCODE used deepTools 1.5.8.1 (Ramírez et al., 2014). Equivalently expressed gene sets were considered as the mean signal of the two genes ranked above and below each gene of interest. Distance to insulators was calculated using BedTools (2.16.2).

Statistical Analysis

Results are presented as means ± SEM. Statistical tests were performed using one-way ANOVA with a Newman-Keuls posttest. Statistical analysis of chromatin color data sets was a chi-square two-tailed analysis. All statistical analysis was done in with GraphPad Prism, unless otherwise noted.

ACCESSION NUMBERS

The RNA-sequencing data sets reported in this article have been deposited in the NCBI Gene Expression Omnibus and are accessible through GEO series accession number GSE62668.

SUPPLEMENTAL INFORMATION

Supplemental information includes Extended Experimental Procedures, three figures, and four tables and can be found with this article online at http://dx.doi.org/10.1016/j.cell.2014.11.005.

AUTHOR CONTRIBUTIONS

A.Ö. and J.A.P. conceived of the study. J.A.P., A.Ö., and A.L. designed the study, supervised all analyses, and wrote the manuscript. A.Ö., A.L., M.W., T.T., and M.D. did all fly work and analyzed the metabolic phenotypes. G.R., M.A., and N.I. contributed to study design and experiments. A.L., C.R., P.M.I., M.D., and A.Ö performed eating behavior and CO2 measurements. A.Ö. and A.L performed immunohistochemistry on fat body cells. A.Ö., A.L., M.W., T.T., U.B., M.S., N.R., and M.R. contributed to generation of the RNaseq data. E.C., S.H., T.V., and L.P. performed the bioinformatic analyses.

ACKNOWLEDGMENTS

This research was supported by the Max-Planck Society, EU (NoE Epigenesys), and the ERC 281641. A.Ö. was supported by Swedish VR K2011-78PK-21893-01-2 and SSMF grants. T.V., L.P., and E.C. were supported by Spanish Ministry grant BFU2011-30246, RYC-2010-07114, Marie Curie European Reintegration Grant "Evo-Chromo," and the IMPPC. C.R. and P.M.I. were supported by the Champalimaud Foundation, the Human Frontiers Program Project Grant RGP0022/2012, and the Portuguese Foundation for Science and Technology (FCT) grant PTDC/BIA-BCM/118684/2010. P.M.I. is supported by the postdoctoral fellowship SFRH/BPD/79325/2011 from the Foundation for Science and Technology. The authors are grateful to P. Georgiev, S. Raja, T. Manke, J. Longinotto, and T. Lu for important technical and theoretical help; to D. Corona, R. Bodmer, H. Esterbauer, and T. Jenuwein for critical discussions; and to H.J. and J.C.P. for everything.

Received: March 25, 2014
Revised: August 27, 2014
Accepted: October 31, 2014
Published: December 4, 2014

REFERENCES

Anderson, L.M., Riffle, L., Wilson, R., Travlos, G.S., Lubomirski, M.S., and Alvord, W.G. (2006). Preconceptional fasting of fathers alters serum glucose in offspring of mice. Nutrition *22*, 327–331.

Anway, M.D., Cupp, A.S., Uzumcu, M., and Skinner, M.K. (2005). Epigenetic transgenerational actions of endocrine disruptors and male fertility. Science *308*, 1466–1469.

Ashe, A., Sapetschnig, A., Weick, E.M., Mitchell, J., Bagijn, M.P., Cording, A.C., Doebley, A.L., Goldstein, L.D., Lehrbach, N.J., Le Pen, J., et al. (2012). piRNAs can trigger a multigenerational epigenetic memory in the germline of C. elegans. Cell *150*, 88–99.

Blondeau, B., Avril, I., Duchene, B., and Bréant, B. (2002). Endocrine pancreas development is altered in foetuses from rats previously showing intra-uterine growth retardation in response to malnutrition. Diabetologia *45*, 394–401.

Braunschweig, M., Jagannathan, V., Gutzwiller, A., and Bee, G. (2012). Investigations on transgenerational epigenetic response down the male line in F2 pigs. PLoS ONE *7*, e30583.

Buescher, J.L., Musselman, L.P., Wilson, C.A., Lang, T., Keleher, M., Baranski, T.J., and Duncan, J.G. (2013). Evidence for transgenerational metabolic programming in Drosophila. Dis. Model. Mech. *6*, 1123–1132.

Burga, A., Casanueva, M.O., and Lehner, B. (2011). Predicting mutation outcome from early stochastic variation in genetic interaction partners. Nature *480*, 250–253.

Carone, B.R., Fauquier, L., Habib, N., Shea, J.M., Hart, C.E., Li, R., Bock, C., Li, C., Gu, H., Zamore, P.D., et al. (2010). Paternally induced transgenerational environmental reprogramming of metabolic gene expression in mammals. Cell *143*, 1084–1096.

Daxinger, L., and Whitelaw, E. (2012). Understanding transgenerational epigenetic inheritance via the gametes in mammals. Nat. Rev. Genet. *13*, 153–162.

Dias, B.G., and Ressler, K.J. (2014). Parental olfactory experience influences behavior and neural structure in subsequent generations. Nat. Neurosci. *17*, 89–96.

Dorus, S., Busby, S.A., Gerike, U., Shabanowitz, J., Hunt, D.F., and Karr, T.L. (2006). Genomic and functional evolution of the Drosophila melanogaster sperm proteome. Nat. Genet. *38*, 1440–1445.

Dunn, G.A., and Bale, T.L. (2009). Maternal high-fat diet promotes body length increases and insulin insensitivity in second-generation mice. Endocrinology *150*, 4999–5009.

Ernst, J., and Kellis, M. (2010). Discovery and characterization of chromatin states for systematic annotation of the human genome. Nat. Biotechnol. *28*, 817–825.

Filion, G.J., van Bemmel, J.G., Braunschweig, U., Talhout, W., Kind, J., Ward, L.D., Brugman, W., de Castro, I.J., Kerkhoven, R.M., Bussemaker, H.J., and van Steensel, B. (2010). Systematic protein location mapping reveals five principal chromatin types in Drosophila cells. Cell *143*, 212–224.

Fullston, T., Ohlsson Teague, E.M., Palmer, N.O., DeBlasio, M.J., Mitchell, M., Corbett, M., Print, C.G., Owens, J.A., and Lane, M. (2013). Paternal obesity initiates metabolic disturbances in two generations of mice with incomplete penetrance to the F2 generation and alters the transcriptional profile of testis and sperm microRNA content. FASEB J. *27*, 4226–4243.

Gapp, K., Jawaid, A., Sarkies, P., Bohacek, J., Pelczar, P., Prados, J., Farinelli, L., Miska, E., and Mansuy, I.M. (2014). Implication of sperm RNAs in transgenerational inheritance of the effects of early trauma in mice. Nat. Neurosci. *17*, 667–669.

Gniuli, D., Calcagno, A., Caristo, M.E., Mancuso, A., Macchi, V., Mingrone, G., and Vettor, R. (2008). Effects of high-fat diet exposure during fetal life on type 2 diabetes development in the progeny. J. Lipid Res. *49*, 1936–1945.

Goodliffe, J.M., Cole, M.D., and Wieschaus, E. (2007). Coordinated regulation of Myc trans-activation targets by Polycomb and the Trithorax group protein Ash1. BMC Mol. Biol. *8*, 40.

Greer, E.L., Maures, T.J., Ucar, D., Hauswirth, A.G., Mancini, E., Lim, J.P., Benayoun, B.A., Shi, Y., and Brunet, A. (2011). Transgenerational epigenetic inheritance of longevity in Caenorhabditis elegans. Nature *479*, 365–371.

Jimenez-Chillaron, J.C., Isganaitis, E., Charalambous, M., Gesta, S., Pentinat-Pelegrin, T., Faucette, R.R., Otis, J.P., Chow, A., Diaz, R., Ferguson-Smith, A., and Patti, M.E. (2009). Intergenerational transmission of glucose intolerance and obesity by in utero undernutrition in mice. Diabetes *58*, 460–468.

Kharchenko, P.V., Alekseyenko, A.A., Schwartz, Y.B., Minoda, A., Riddle, N.C., Ernst, J., Sabo, P.J., Larschan, E., Gorchakov, A.A., Gu, T., et al. (2011). Comprehensive analysis of the chromatin landscape in Drosophila melanogaster. Nature *471*, 480–485.

Kiani, J., Grandjean, V., Liebers, R., Tuorto, F., Ghanbarian, H., Lyko, F., Cuzin, F., and Rassoulzadegan, M. (2013). RNA-mediated epigenetic heredity requires the cytosine methyltransferase Dnmt2. PLoS Genet. *9*, e1003498.

Klimcáková, E., Roussel, B., Márquez-Quiñones, A., Kovácová, Z., Kovácíková, M., Combes, M., Siklová-Vítková, M., Hejnová, J., Srámková, P., Bouloumié, A., et al. (2011). Worsening of obesity and metabolic status yields similar molecular adaptations in human subcutaneous and visceral adipose tissue: decreased metabolism and increased immune response. J. Clin. Endocrinol. Metab. *96*, E73–E82.

Koza, R.A., Nikonova, L., Hogan, J., Rim, J.S., Mendoza, T., Faulk, C., Skaf, J., and Kozak, L.P. (2006). Changes in gene expression foreshadow diet-induced obesity in genetically identical mice. PLoS Genet. *2*, e81.

Kucherenko, M.M., Marrone, A.K., Rishko, V.M., Magliarelli, Hde.F., and Shcherbata, H.R. (2011). Stress and muscular dystrophy: a genetic screen for dystroglycan and dystrophin interactors in Drosophila identifies cellular stress response components. Dev. Biol. *352*, 228–242.

Lee, Y.H., Nair, S., Rousseau, E., Allison, D.B., Page, G.P., Tataranni, P.A., Bogardus, C., and Permana, P.A. (2005). Microarray profiling of isolated abdominal subcutaneous adipocytes from obese vs non-obese Pima Indians: increased expression of inflammation-related genes. Diabetologia *48*, 1776–1783.

Lee, H.C., Gu, W., Shirayama, M., Youngman, E., Conte, D., Jr., and Mello, C.C. (2012). C. elegans piRNAs mediate the genome-wide surveillance of germline transcripts. Cell *150*, 78–87.

Lundberg, L.E., Stenberg, P., and Larsson, J. (2013). HP1a, Su(var)3-9, SETDB1 and POF stimulate or repress gene expression depending on genomic position, gene length and expression pattern in Drosophila melanogaster. Nucleic Acids Res. *41*, 4481–4494.

Merico, D., Isserlin, R., Stueker, O., Emili, A., and Bader, G.D. (2010). Enrichment map: a network-based method for gene-set enrichment visualization and interpretation. PLoS ONE *5*, e13984.

Morgan, H.D., Sutherland, H.G., Martin, D.I., and Whitelaw, E. (1999). Epigenetic inheritance at the agouti locus in the mouse. Nat. Genet. *23*, 314–318.

Nègre, N., Brown, C.D., Shah, P.K., Kheradpour, P., Morrison, C.A., Henikoff, J.G., Feng, X., Ahmad, K., Russell, S., White, R.A., et al. (2010). A comprehensive map of insulator elements for the Drosophila genome. PLoS Genet. *6*, e1000814.

Nègre, N., Brown, C.D., Ma, L., Bristow, C.A., Miller, S.W., Wagner, U., Kheradpour, P., Eaton, M.L., Loriaux, P., Sealfon, R., et al. (2011). A cis-regulatory map of the Drosophila genome. Nature *471*, 527–531.

Ng, S.F., Lin, R.C., Laybutt, D.R., Barres, R., Owens, J.A., and Morris, M.J. (2010). Chronic high-fat diet in fathers programs β-cell dysfunction in female rat offspring. Nature *467*, 963–966.

Ozanne, S.E., Wang, C.L., Dorling, M.W., and Petry, C.J. (1999). Dissection of the metabolic actions of insulin in adipocytes from early growth-retarded male rats. J. Endocrinol. *162*, 313–319.

Paredes, S., Branco, A.T., Hartl, D.L., Maggert, K.A., and Lemos, B. (2011). Ribosomal DNA deletions modulate genome-wide gene expression: "rDNA-sensitive" genes and natural variation. PLoS Genet. *7*, e1001376.

Patti, M.E. (2013). Intergenerational programming of metabolic disease: evidence from human populations and experimental animal models. Cell. Mol. Life Sci. *70*, 1597–1608.

Phalke, S., Nickel, O., Walluscheck, D., Hortig, F., Onorati, M.C., and Reuter, G. (2009). Retrotransposon silencing and telomere integrity in somatic cells of Drosophila depends on the cytosine-5 methyltransferase DNMT2. Nat. Genet. *41*, 696–702.

Pietiläinen, K.H., Naukkarinen, J., Rissanen, A., Saharinen, J., Ellonen, P., Keränen, H., Suomalainen, A., Götz, A., Suortti, T., Yki-Järvinen, H., et al. (2008). Global transcript profiles of fat in monozygotic twins discordant for BMI: pathways behind acquired obesity. PLoS Med. *5*, e51.

Radford, E.J., Ito, M., Shi, H., Corish, J.A., Yamazawa, K., Isganaitis, E., Seisenberger, S., Hore, T.A., Reik, W., et al. (2014). In utero undernourishment perturbs the adult sperm methylome and intergenerational metabolism. Science *345*. Published online July 10, 2014. http://dx.doi.org/10.1126/science.1255903.

Ramírez, F., Dündar, F., Diehl, S., Grüning, B.A., and Manke, T. (2014). deepTools: a flexible platform for exploring deep-sequencing data. Nucleic Acids Res. *42* (Web Server issue), W187–W91.

Rando, O.J. (2012). Daddy issues: paternal effects on phenotype. Cell *151*, 702–708.

Rassoulzadegan, M., Grandjean, V., Gounon, P., Vincent, S., Gillot, I., and Cuzin, F. (2006). RNA-mediated non-mendelian inheritance of an epigenetic change in the mouse. Nature *441*, 469–474.

Rechavi, O., Houri-Ze'evi, L., Anava, S., Goh, W.S., Kerk, S.Y., Hannon, G.J., and Hobert, O. (2014). Starvation-induced transgenerational inheritance of small RNAs in C. elegans. Cell *158*, 277–287.

Ritossa, F.M., Atwood, K.C., and Spiegelman, S. (1966). A molecular explanation of the bobbed mutants of Drosophila as partial deficiencies of "ribosomal" DNA. Genetics *54*, 819–834.

Schotta, G., Lachner, M., Sarma, K., Ebert, A., Sengupta, R., Reuter, G., Reinberg, D., and Jenuwein, T. (2004). A silencing pathway to induce H3-K9 and H4-K20 trimethylation at constitutive heterochromatin. Genes Dev. *18*, 1251–1262.

Seong, K.H., Li, D., Shimizu, H., Nakamura, R., and Ishii, S. (2011). Inheritance of stress-induced, ATF-2-dependent epigenetic change. Cell *145*, 1049–1061.

Shirayama, M., Seth, M., Lee, H.C., Gu, W., Ishidate, T., Conte, D., Jr., and Mello, C.C. (2012). piRNAs initiate an epigenetic memory of nonself RNA in the C. elegans germline. Cell *150*, 65–77.

Skorupa, D.A., Dervisefendic, A., Zwiener, J., and Pletcher, S.D. (2008). Dietary composition specifies consumption, obesity, and lifespan in Drosophila melanogaster. Aging Cell *7*, 478–490.

Teleman, A.A., Hietakangas, V., Sayadian, A.C., and Cohen, S.M. (2008). Nutritional control of protein biosynthetic capacity by insulin via Myc in Drosophila. Cell Metab. *7*, 21–32.

Voigt, A., Agnew, K., van Schothorst, E.M., Keijer, J., and Klaus, S. (2013). Short-term, high fat feeding-induced changes in white adipose tissue gene expression are highly predictive for long-term changes. Mol. Nutr. Food Res. *57*, 1423–1434.

Waterland, R.A., Dolinoy, D.C., Lin, J.R., Smith, C.A., Shi, X., and Tahiliani, K.G. (2006). Maternal methyl supplements increase offspring DNA methylation at Axin Fused. Genesis *44*, 401–406.

Whitelaw, N.C., Chong, S., and Whitelaw, E. (2010). Tuning in to noise: epigenetics and intangible variation. Dev. Cell *19*, 649–650.

Wolff, G.L., Kodell, R.L., Moore, S.R., and Cooney, C.A. (1998). Maternal epigenetics and methyl supplements affect agouti gene expression in Avy/a mice. FASEB J. *12*, 949–957.

Xing, Y., Shi, S., Le, L., Lee, C.A., Silver-Morse, L., and Li, W.X. (2007). Evidence for transgenerational transmission of epigenetic tumor susceptibility in Drosophila. PLoS Genet. *3*, 1598–1606.